Atmos. Chem. Phys. Discuss.,
doi:10.5194/acp-2016-247-AC1, 2016

Atmospheric Chemistry and Physics Discussions

Interactive comment on "Heterogeneous Kinetics of H_2O, HNO_3 and HCl on HNO_3 hydrates (α-NAT, β-NAT, NAD) in the range 175–200 K" *by* Riccardo Iannarelli and Michel J. Rossi

Riccardo Iannarelli and Michel J. Rossi

michel.rossi@psi.ch

Received and published: 27 July 2016

Answers to Question of Referee 1:

Q2- Page 7, line 185, silicon has a cutoff of 1500 cm-1 in the FTIR so how can the range extend from 4000-700 cm-1?

See Figure 1a, 1b.

Fig. 1a: Absorption spectrum of Si window (commercially available material from Nicodom sro)

Fig. 1b: Taken from the Handbook of Optics (Optical Society of America, McGraw-Hill

book Co. 1978)

A2- Figures 1a and 1b present transmission curves of Si windows that always have a very thin coating (on the order of 50-100 nm) SiO2 that protects the bulk of Si from oxidation. Although transmission is reduced in the 1500 to 600 nm range it is sufficiently transmitting to enable high-quality absorption spectra to be recorded. In our case the DIGILAB FTS 575 provides high throughput thanks to its 3" collection optics. The centerburst signal reduces from 9V to 3V after passage across 2a pair of 5mm thick KCl and a 2.0 mm thick Si window with external location of the HgCdTe detector cooled at 77 K.

Q3- Page 8, lines 219-220, the authors discuss that the transition in phases was observed via FTIR yet no FTIR or MS spectra were shown in the entire 52 pages of the manuscript. It would be interesting to the readers to show sample spectra and also to mention in a table the m/z and the wavenumbers where hydrates, HNO3, HCl and water were observed.

A3- We agree with the referee regarding the presentation of raw FTIR/MS data of the discussed ternary HNO3/HCl/H2O chemical systems. To this effect we have added two new Figures (6 and 7) displaying combined FTIR/MS sample data as well as corresponding Table 3. However, for the binary system HNO3/H2O we have presented the corresponding combined sample FTIR absorption/MS data already in the Iannarelli and Rossi (2015) publication (J. Geophys. Res. 120, 11707-11727, 2015) such that renewed presentation in the present context would appear not to be appropriate. We therefore point out this reference when discussing the thermodynamic and kinetic data of the simple binary HNO3/H2O system.

TEXT- We refrain at this point from showing raw data (FTIR absorption spectra and MS data as a function of time) because representative samples have been shown by Iannarelli and Rossi (2015) for alpha- and beta-NAT. We will defer the presentation of raw data on the interaction of HCl on alpha- and beta-NAT to Section 3.3 below.

The following text is introduced into chapter 3.3 which introduces the ternary HCl/HNO3/H2O system.

TXT- Figure 6 displays raw data from repetitive pulsed dosing of HCl onto an ïĄą-NAT/ice substrate as a function of elapsed time. The individual pulses, of which there were twelve and identifiable by sharp peaks on top of the red columns in the lower panel displaying the MS signals of HCl (red, m/e 36), H2O (blue, m/e 18) and HNO3 (black, m/e 46) corresponded to (4-5) x 1016 molecule per pulse resulting in a total HCl dose of approximately 3 x 1017 molecules. This is the dose effectively administered to the alpha-NAT when the fraction of HCl going to the vessel walls and escaping the SFR has been subtracted. This dose approximately corresponds to 1000 molecular monolayers of HCl adsorbed onto the substrate. The temperature of the cryostat is displayed as the green trace in the lower panel, and with every T-increase the MS steady-state levels of HCl, H2O and HNO3 increase concomitantly. (During the pulsed admission of HCl the MS levels of HNO3 and H2O are subject to artifacts owing to rapid switching). Turning to the upper panel of Figure 6 we display a series of FTIR transmission spectra from 700 to 4000 cm-1 at specific times during the repetitive pulsing experiment which are indicated in the lower panel by a series of color-coded “sp1” and continuing going from red to purple. The principal peak positions have been collected in Table 3 and will be discussed below in terms of changes in the “pure” alpha-NAT/ice absorption spectra owing to the presence of increasing adsorbed HCl. The enlarged IR-spectral range in the upper panel of Figure 6 displays the effect of the HCl adsorption particularly well by showing a non-monotonic sequence of IR absorption peaks not present in the “pure” reference spectra from Iannarelli and Rossi (2015). The raw MS data from the lower panel of Figure 6 have been used to calculate the kinetic and thermodynamic data displayed in Figure 8.

Figure 7 displays raw data from repetitive pulsed dosing of HCl onto a ïĄć-NAT/ice substrate in analogy to Figure 6. The eleven individual pulses corresponded to (6-7) x 1016 molecule per pulse resulting in a total HCl dose of approximately 4 x 1017

molecules which amounts to 1300 molecular monolayers or so. Like in Figure 6 the upper panel displays a series of color-coded FTIR absorption spectra in transmission with the principal peak positions collected in Table 3. As for Figure 6 the MS steady-state levels at the different temperatures will be used to derive the kinetic and thermodynamic data of Figure 9 as a function of temperature. In addition, Figure S6 presents an enlarged graph for the non-exponential decay of a HCl pulse interacting with both ïĄą- and ïĄć-NAT on a 30 s time scale consisting of a fast and a slowly-decaying portion. The evaluation of such pulsed admission MS signals has been presented in the past (Iannarelli and Rossi, 2014, Supplemental Information (SI)) and the present analysis and fitting of the HCl MS signals follows the same scheme.

A look at Table 3 should provide an answer as to whether or not there is an identifiable spectral fingerprint of HCl adsorbed on alpha-or beta-NAT in the FTIR absorption spectrum of the combined alpha- or beta-NAT/HCl system displayed in Figures 6 and 7. The first column of Table 3 reveals the spectral fingerprint of HCl for alpha-NAT/HCl in terms of additional peaks (in italics) that are not present in the reference spectrum (pure ïĄą-NAT) recorded using the identical instrument and presented in the third column. There seem to be two spectral regions where the presence of HCl may be apparent, namely in the 1618-1644 cm-1 region corresponding to the broad bending vibration of the proton-ordered waters of hydration (Ritzhaupt and Devlin, 1991; Martin-Llorente et al., 2006), and more importantly, the band at 1328 cm-1 that overlaps with the 1339 cm-1 vibration, the latter of which is not changing with increasing HCl dose. The series of FTIR absorption spectra displayed in Figure 6 shows the non-monotonous change of intensity at this transition (1328 cm-1): sp1 (red), sp2 (yellow) and sp3 (green) display the growth of a shoulder to the red of the 1375 cm-1 peak, sp4 (turquoise), sp5 (blue) and sp6 (purple) show the separate peak in its decline (1328 cm-1) owing to evaporation of HCl together with NAT. For beta-NAT the analogous situation is displayed in the second and fourth column of Table 3 and Figure 7. Here the presence of HCl is more discrete within the FTIR absorption spectrum of beta-NAT as Table 3 suggests the well-separated peak to the blue of the 3227 cm-1 ice peak at 3360 cm-1 to be a

HCl tracer as it looks very similar to the HCl/H2O system (Iannarelli and Rossi, 2014; Chiesa and Rossi, 2013). The peaks identified to appear in the FTIR spectrum upon HCl adsorption may be found in the fifth column of Table 3 which displays the principal IR peaks in the reference HCl/H2O system, except the 1200 cm-1 vibration found in column 1 and 2 whose origin remains unclear.

Q4- Page 13, lines 369-372, the authors discussed the difference between Alpha-NAT and HCl; yet no HCl results were shown in Figure 2.

A4- The purpose of that statement regarding the difference between Rev(H2O) in the HCl vs. the HNO3 hydrate was to alert the reader to a significant difference between the two hydrates. We have inserted the two references that deal with the HCl hydrates (amorphous HCl hydrate and HCl Hexahydrate).

TXT- This result is very different compared to the previously studied case of HCl amorphous and crystalline hexahydrate using the same apparatus (Iannarelli and Rossi, 2013), where the evaporation of H2O takes place at a rate characteristic of pure ice despite the presence of adsorbed HCl on the ice and is in agreement with the findings of Delval and Rossi (2005).

Q5- Page 14, line 421, can the authors comment how the relative errors were calculated and why same error in PV (30%) and TO (60%) experiments were observed on both the NAT and NAD films?

A5- Although preferred from the point of view of avoiding sample saturation, we attribute twice the uncertainty to the TO compared to the PV technique. TO involves taking a difference of two large numbers in the denominator of Equations (7) and (8), which is the reason to attribute a larger experimental uncertainty to this method.

TXT- The largest uncertainty in our experiment is that of the flow rate introduced into the reactor, which is assigned a relative error of 25%. The flow rate measurement affects the calibration of the MS and therefore the measurement of all the concentrations in

the reactor (Eq. 4). Therefore, we estimate a global relative error of 30% for PV experiments and double this uncertainty for TO experiments because Equations (7) and (8) imply a difference of two large numbers in many cases, as discussed above. We therefore assign a global 60% relative error to results obtained in TO experiments.

Q6- Page 15, lines 448-453, again the authors talk about comparisons to HCl experiments however no HCl data are present in Figure 4b. Which figure the authors want the reader to check to compare HCl case to figure 4a, please mention the figure since HCl experiments are introduced in the next Section.

A6- As discussed above for alpha-NAT we are referring to a previous study on the BINARY HCl/H2O phase (Iannarelli and Rossi, 2013) whereas chapter 3.3 below deals with the TERNARY HCl/HNO3/H2O system.

TXT- As in the case of alpha-NAT, this result is very different compared to the case of HCl hydrates studied before using the same apparatus (Iannarelli and Rossi, 2013) where the evaporation of H2O is not influenced by the presence of adsorbed HCl on the ice and takes place at a rate characteristic of pure ice for all HCl concentrations used.

Q7- Page 17, lines 484-488, why are the authors making assumptions regarding the substrates can't they get information on changes due to HCl from FTIR?

A7- In response to your discussion point 3 above we have introduced Figures 6 and 7 displaying FTIR absorption spectra in the presence of HCl whose principal peak positions have been collected in the new Table 3 (not reproduced here but included in the new manuscript version). Regarding the ternary HCl/HNO3/H2O system treated here we had to make some verified assumptions in order to keep the experimental parameter space to an acceptable level. All three simplifying assumptions have been verified in the current laboratory experiments.

TXT- In order to restrain the number of independent measurements on this ternary

system to a practical level we had to make some assumptions and/or simplifications in order to measure the unknown parameters of Eq. (2) for each gas used. Specifically, we made the following reasonable assumptions, both for alpha-NAT and beta-NAT substrates which have been experimentally verified in laboratory experiments:

Q8- Page 18, lines 534-535, the authors mentioned a decrease in ïAËŻaËŻ-ïAËŻc′-NAT as a function of increasing temperature but looking at figure 7a it looks like there was no change in the signal within experimental error.

A8- Figure 9a in fact shows a slight decrease of the HCl accommodation coefficient on beta-NAT similar to alpha-NAT (Figure 8a) where the decrease is a little larger over a similar T-range. However, as the referee suggests it may or may not be significant for beta-NAT.

TXT- . . .decreases as a function of temperature in the range 177-201 K, varying from 0.025 at 177 K to 0.016 at 201 K which may or may not be significant.

Q9- Page 19, lines 563-574 are the two distinct temperature regimes in Figure 2a due to surface disorder on ice?

A9- We certainly suggest this to be due to contamination-induced surface disorder that is discussed in the next few paragraphs and that has been highlighted in the studies of McNeill et al. However, at this point this remains a suggestion because we do not have structural proof of this hypothesis because in the present case the term “multidiagnostic” does not extend the investigation to structural studies.

Q10- Page 24, lines 704-709 why only TO experiments were possible for HNO3? This point is not so clear.

A10- The answer to this question has been given in Section 2.2, line 275-279.

Q11- Page 25, lines 753-758 can the authors comment why their results for HCl experiments were different from those by Haynes (2002)?

A11- We have the suspicion that the difference has to do with the fact that Hynes et al. (2002) performed their experiments at significantly higher temperatures which possible enables reversibility. This is mentioned on pg. 28, lines 834-837.

Q12- Figures 2-7 although the C2 authors mentioned the symbols in the text but it was so confusing to keep going back and forth between the text and the figure given the extra length of this manuscript and the different systems studied. I recommend that the authors explain the symbols in the caption for every figure.

A12- The captions have been written according to the guidelines of ACP. Owing to the complexity of the Figures we have added explanation of the symbols inside the Figures.

Interactive comment on Atmos. Chem. Phys. Discuss., doi:10.5194/acp-2016-247, 2016.

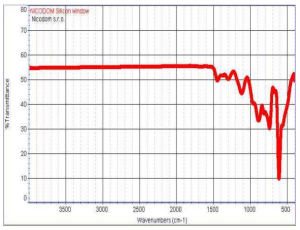

Figure 1a (Caption in Report)

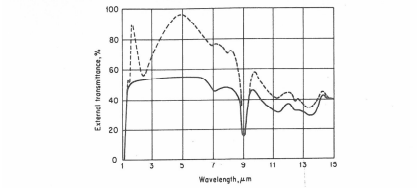

Fig. 125 Transmission of silicon, thickness 2.5 mm. Dashed curve is for a sample coated to reduce reflection loss. [*From Texas Instruments (no date).*]

Figure 1b (Caption in Report)

Fig. 1. Fig1a,1b and 2 for Answers to Referee1 and Referee2